Simulation of Liesegang Patterns: Effect of Reversible Complex Formation of Precipitate

István Lagzi*

Department of Physical Chemistry, Eötvös University, Budapest, Hungary

Received: July 24, 2003; In Final Form: October 8, 2003

Formation of 1D Liesegang patterns was studied numerically by assuming precipitation and reversible complex formation. The Ostwald's supersaturation model reported by Büki, Kárpáti-Smidróczki, and Zrínyi (BKZ model) was developed and extended further. The position of the first and last bands measured from the junction point of the inner and outer electrolytes is linearly proportional to the square root of its formation time for the different initial concentrations of inner electrolyte (β_o). The propagation of patterns along the diffusion column is slower at higher β_o. The correlation between the distance of the first and last bands measured from the beginning of the diffusion column is strictly linear. The variation of the total number of bands with β_o has a maximum. The presented model reproduces the moving precipitate zones and nonlinear oscillation of the total number of bands in time due to the complex formation of the precipitate.

1. Introduction

A Liesegang pattern is a typical example of the spatiotemporal pattern formation of reaction−diffusion systems and the phenomenon has been studied for a long time. Investigation of the features of the classical Liesegang system[1] showed that the variation of the total number of bands (N) increases monotonically with time. The regular pattern formation has four significant empirical regularities (the spacing law,[2] the time law,[3] the width law[4−6] and the Matalon−Packter law[7,8]). The time law is $X_n \propto t_n^{1/2}$, where X_n is the position of the nth band measured from the junction point of two electrolytes and t_n is the time of appearance of the nth band. This law reflects the diffusive behavior of the outer electrolyte into a gel.

In several cases precipitate zones can redissolve in excess invading electrolyte due to the complex formation of precipitate. This effect causes a propagating precipitate pattern along the diffusion column. Such experiments were carried out in NaOH/Cr(NO$_3$)$_3$,[9−11] where Cr(OH)$_3$ redissolved in excess OH$^-$ produces [Cr(OH)$_4$]$^-$, and in the KI/HgCl$_2$ system,[12] where HgI$_2$ forms [HgI$_4$]$^{2-}$ by redissolution in excess I$^-$. Recently, Sultan and co-workers presented experimental studies of some features and characteristics of the NH$_4$OH/CoCl$_2$/gelatine system,[13−17] where the formed precipitate Co(OH)$_2$(s) reacts with NH$_4$OH, yielding [Co(NH$_3$)$_6$]$^{2+}$. Precipitation and complex formation produce moving strata bands down the tube and exhibit a deterministic chaotic variation of the total number of bands in time. They also found that the positions of the first band (d_{fb}) and the last band (d_{lb}) as measured from the gel surface both have a square root dependence in time and that there is a linear correlation between these two variables.[15] The numerical model of Al-Ghoul and Sultan[18,19] contains irreversible complex formation, whereas reversible complex formation of the precipitate was not included. They adopted the model of Polezhaev and Müller[20] to describe the Liesegang pattern formation. The numerical simulation reproduced only some basic aspects of their experiments and they reported that the simulated correlation between d_{fb} and d_{lb} is not perfectly linear.[18] In the numerical study, the motion of the pattern, the nonlinear oscillation of N

and other features that were demonstrated in the experimental work[14,15] was not investigated.

The aim of this paper is to study all qualitative features of the precipitation and reversible complex formation scenarios observed in experiments[14,15] using numerical simulation methods.

2. Model

The description of the formation of precipitate used was based on Ostwald's supersaturation theory[21] as presented by Büki et al.[22,23] This approach involves two thresholds, one for the nucleation and one for the autocatalytic precipitate growth.[22,23] The nucleation can occur only in a supersaturated state, but when the nuclei are present, the precipitation process is fast. The system is normally highly supersaturated and therefore the precipitation reaction is practically irreversible. The skeleton mechanism of a simple precipitation and reversible complex formation is

$$A^+(aq) + B^-(aq) \rightarrow P(s) \tag{1}$$

$$P(s) + D(aq) \rightarrow C(aq) \tag{2}$$

$$C(aq) \rightarrow P(s) + D(aq) \tag{3}$$
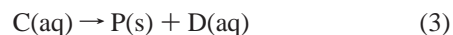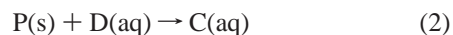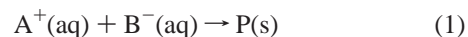
where A$^+$(aq) and B$^-$(aq) are the ionic species (the outer and the inner electrolytes, respectively), P(s) is the precipitated product, D(aq) is the complex former species, and C(aq) is the complex. Precipitation is faster than the other reaction rates of the model. We supposed that the complex former species (D(aq)) diffuses into a diffusion column with the outer electrolyte (A$^+$(aq)), which has same initial concentration as the outer electrolyte. This assumption differs from that applied by Al-Ghoul and Sultan.[18,19] In their model, the complex former species (NH$_4^+$) is an intermediate, which forms from the precipitation process, and its initial concentration is assumed to be zero in the diffusion column. The presented mechanism (1)−(3) is a possible simplified model of the NH$_4$Cl/AgNO$_3$

Simulation of Liesegang Patterns

J. Phys. Chem. B, Vol. 107, No. 49, 2003 **13751**

system, where the formed precipitate AgCl reacts with ammonia producing $Ag(NH_3)_2^+$.

The 1D Liesegang system is governed by the following set of partial differential equations:

$$\frac{\partial \alpha}{\partial \tau} = D_\alpha \frac{\partial^2 \alpha}{\partial x^2} - \Delta(K_s, L, \alpha\beta) \tag{4}$$

$$\frac{\partial \beta}{\partial \tau} = D_\beta \frac{\partial^2 \beta}{\partial x^2} - \Delta(K_s, L, \alpha\beta) \tag{5}$$

$$\frac{\partial \gamma}{\partial \tau} = D_\gamma \frac{\partial^2 \gamma}{\partial x^2} + \kappa_2 \pi \delta - \kappa_3 \gamma \tag{6}$$

$$\frac{\partial \delta}{\partial \tau} = D_\delta \frac{\partial^2 \delta}{\partial x^2} - \kappa_2 \pi \delta + \kappa_3 \gamma \tag{7}$$

$$\frac{\partial \pi}{\partial \tau} = \Delta(K_s, L, \alpha\beta) - \kappa_2 \pi \delta + \kappa_3 \gamma \tag{8}$$

where α, β, γ, and δ are the dimensionless concentrations and D_α, D_β, D_γ, and D_δ are the dimensionless diffusion coefficients of $A^+(aq)$, $B^-(aq)$, $C(aq)$, and $D(aq)$, respectively, π is the dimensionless amount of precipitate product $P(s)$. κ_2 and κ_3 are the dimensionless chemical rate constants for reactions (2) and (3). τ is the dimensionless time, x is the dimensionless length. The function $\Delta(K_s, L, \alpha\beta)$ is defined by the following equations:

if $\pi = 0$ (there is no precipitate at the grid point)

$$\Delta(K_s, L, \alpha\beta) = \Sigma_P \theta(\alpha\beta - K_s) \tag{9}$$

if $\pi \neq 0$ (there is some precipitate at the grid point)

$$\Delta(K_s, L, \alpha\beta) = \Sigma_P \theta(\alpha\beta - L) \tag{10}$$

where L is the precipitation product, K_s is the nucleation product, θ is the Heaviside step function, and Σ_P is the amount of the precipitate, which can be formed. For an AB type precipitate this can be calculated on the basis of the following algebraic equation proposed by Büki et al.:[22,23]

$$\Sigma_P = 0.5((\alpha + \beta) - ((\alpha + \beta)^2 - 4(\alpha\beta - L))^{1/2}) \tag{11}$$

The precipitate growth does not continue if π reaches a maximal value (π_{max}) at the grid point. Partial differential equations (4)−(8) were solved numerically using a forward Euler method with boundary conditions:

$$\frac{\partial \alpha}{\partial x}\bigg|_{x=l} = \frac{\partial \beta}{\partial x}\bigg|_{x=l} = \frac{\partial \beta}{\partial x}\bigg|_{x=0} = \frac{\partial \gamma}{\partial x}\bigg|_{x=l} = \frac{\partial \gamma}{\partial x}\bigg|_{x=0} = \frac{\partial \delta}{\partial x}\bigg|_{x=l} = 0 \tag{12}$$

$$\alpha|_{x=0} = \alpha_o \tag{13}$$

$$\delta|_{x=0} = \delta_o \tag{14}$$

where l is the length of the diffusion column and $\alpha_o = \delta_o = 60.0$. The following parameter set was used in the simulations: $D_\alpha = D_\beta = D_\gamma = D_\delta = 0.4$, $L = 0.100$, $K_s = 0.101$, $\kappa_2 = 1 \times 10^{-4}$, $\kappa_3 = 1 \times 10^{-8}$, $l = 3360$, and $\pi_{max} = 5.0$. The following
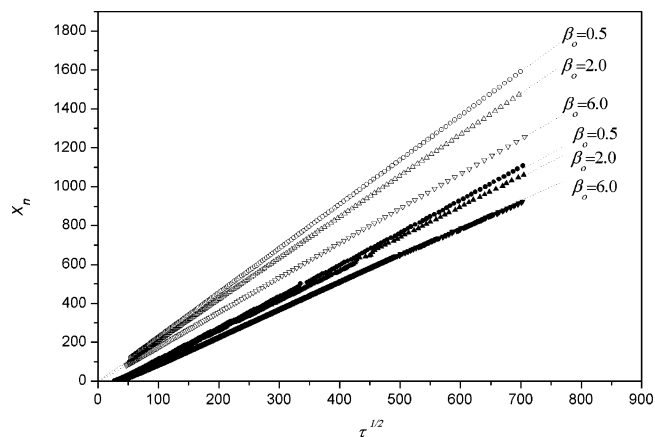

Figure 1. Variation of the positions of the first and last bands measured from the junction point of the inner and outer electrolytes with the square root of time for different values of β_o. The dotted lines represent the fitted linear curves. The open and filled symbols correspond to last and first bands, respectively.
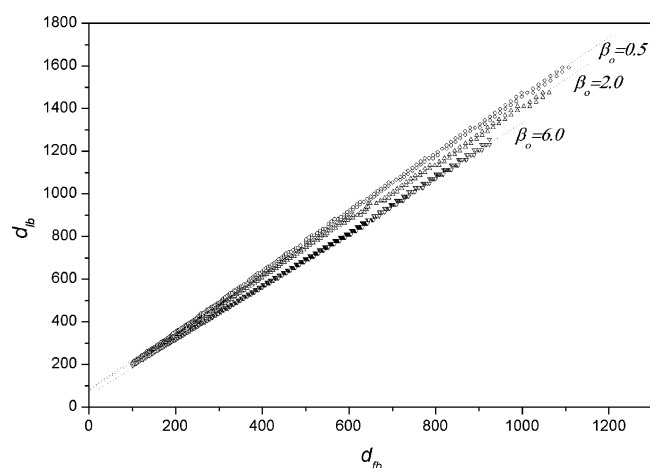

Figure 2. Correlation plot of the distance of the last band versus the first band measured from the junction point of the inner and outer electrolytes at different values of β_o. The dotted lines represent the fitted linear curves.

initial conditions for the concentrations were used:

$$\alpha(\tau=0, x) = \alpha_o \theta(-x) \tag{15}$$

$$\beta(\tau=0, x) = \beta_o \theta(x) \tag{16}$$

$$\delta(\tau=0, x) = \delta_o \theta(-x) \tag{17}$$

$$\pi(\tau=0, x) = \gamma(\tau=0, x) = 0 \tag{18}$$

where β_o was varied between 0.5 and 10.0 in the simulations. The grid spacing and the time step were $\Delta x = 0.8$ and $\Delta \tau = 0.05$, respectively.

3. Results

Figure 1 shows the position of the first and the last bands measured from the junction point of the inner and outer electrolytes as a function of the square root of time. The results suggest that the position of the first and the last bands due to the formation and reversible dissolution of the bands can be described with time by the function $X_n = c_1 \tau_n^{1/2} + c_2$, respectively; i.e., the time law describes not only the evolution of the last but also the first bands in time. The width of the migrating band system (the distance between last and first zones)
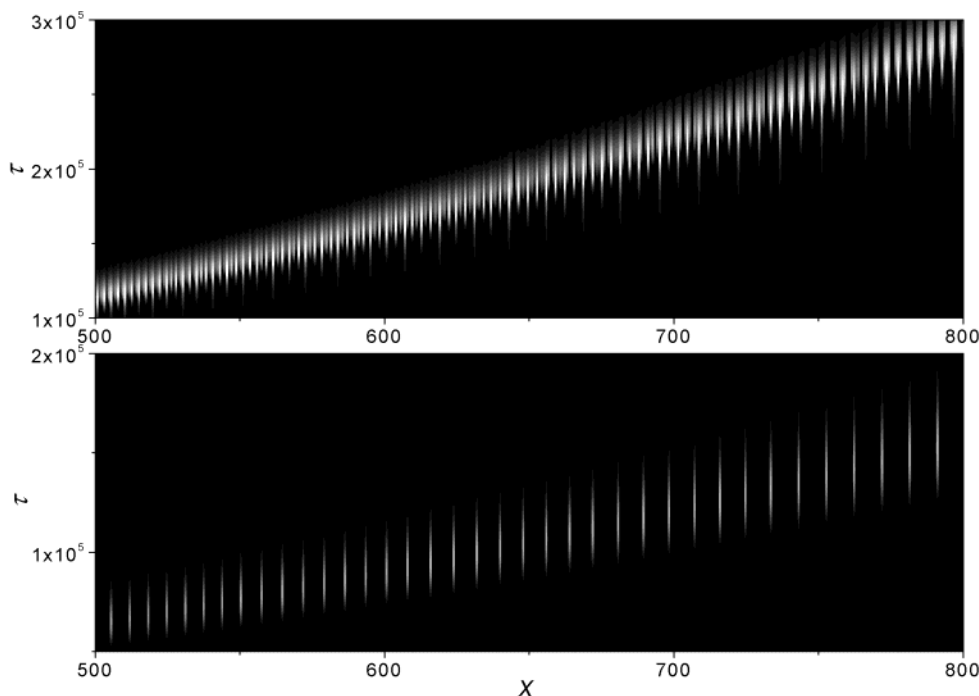
Figure 3. Evolution of 1D Liesegang patterns for various β_o: $\beta_o = 1.0$ (bottom), $\beta_o = 6.0$ (top). The white lines represent the amount of the precipitate.
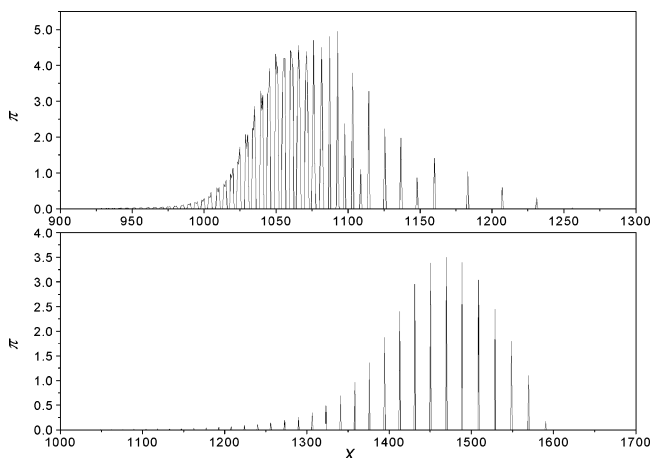

Figure 4. Spatial distribution of amount of precipitate measured from the junction point of the electrolytes for the two different values of β_o: $\beta_o = 1.0$ (bottom), $\beta_o = 6.0$ (top) at $\tau = 5 \times 10^5$.

Figure 5. Variation of the total number of bands with time for different values of β_o: $\beta_o = 1.0$ (bottom), $\beta_o = 6.0$ (top).

TABLE 1: Dependence of the Total Number of Bands (N) on Initial Concentration β_o at $\tau = 4 \times 10^5$

β_o	0.5	1.0	2.0	3.0	4.0	5.0	6.0	7.0	8.0	9.0	10.0
N	31	32	42	40	55	51	50	53	33	22	22

increases linearly with the square root of time. A band was considered present if the amount of precipitate at the grid point was higher than or equal to 0.01 ($\pi \geq 0.01$). The propagation of patterns along the diffusion column is slower at higher β_o.

The plot of the position of the last band (d_{lb}) versus the position of the first band (d_{fb}) shows a strong linear dependence, as shown in Figure 2. This is in good agreement with the experimental results[15] and a better correlation between them is obtained than with the numerical simulation by Al-Ghoul and Sultan, which was not perfectly linear.[18] The spatiotemporal evolutions of Liesegang patterns are illustrate in Figure 3. The patterns map demonstrates well the pattern propagation and the more complex pattern formation behavior in the case of $\beta_o = 6.0$. The distribution of precipitate (π) in space is presented in Figure 4. The amount of the precipitate demonstrates almost Gaussian characteristics in space. The pattern propagation and Gaussian distribution are due to the dissolution of bands behind the pattern (complex formation of the precipitate) and the formation of new ones by precipitation in front of the pattern.
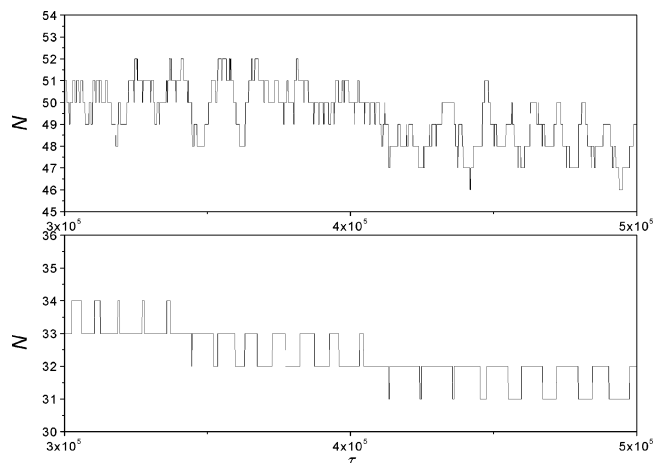
Table 1 presents the dependence of the total number of bands (N) on various initial concentrations of the inner electrolyte (β_o) at the same simulation time. N increases to a maximum value then decreases with β_o. This result coincides with the result reported by Sultan and Sadek.[14]

The most important and interesting behavior of the precipitation and dissolution of the precipitate systems is the nonlinear variation of the total number of bands in time. This main feature was reproduced by the model using reversible complex formation of the precipitate as displayed in Figure 5. It shows that the amplitude of the time oscillation in time is higher at $\beta_o = 6.0$; therefore the nonlinearity is conspicuous in this case.

4. Conclusions

This study focused on the numerical simulation of migrating Liesegang patterns. The numerical model was based on Ost-

Simulation of Liesegang Patterns

J. Phys. Chem. B, Vol. 107, No. 49, 2003 **13753**

wald's supersaturation theory coupled with reversible complex formation due to the reaction of the precipitate product with a complexing agent. A different chemical model and different initial conditions were used than those applied by Al-Ghoul and Sultan.[18,19] The model simulations demonstrate all features that were present experimentally.[14,15,17] The novel features of numerical simulations are follows:

1. The correlation between the position of the first and last bands is strongly linear, as was observed experimentally.[14,17]

2. The spatial distribution of the precipitate exhibits Gaussian characteristics.

3. The total number of bands increases to a maximum value and then decreases as β_o is increased. This is similar to results from the experimental work.[14]

4. The variation of the total number of bands showed nonlinear oscillation behavior in time.[14,15,17]

References and Notes

(1) Liesegang, R. E. *Naturwiss. Wochenschr.* **1896**, *11*, 353.

(2) Jablczynski, K. *Bull. Soc. Chim. Fr.* **1923**, *33*, 1592.

(3) Morse H. W.; Pierce G. W. *Proc. Am. Acad. Arts. Sci.* **1903**, *38*, 625.

(4) Müller, S. C.; Kai, S.; Ross. J. *J. Phys. Chem.* **1982**, *86*, 4078.

(5) Pillai, K. M.; Vaidyan, V. K.; Ittyachan, M. A. *Colloid. Polym. Sci.* **1980**, *258*, 831.

(6) Droz, M.; Magnin, J.; Zrinyi, M. *J. Chem. Phys.* **1999**, *110*, 9618.

(7) Matalon, R.; Packter, A. *J. Colloid Sci.* **1955**, *10*, 46.

(8) Antal, T.; Droz, M.; Magnin, J.; Rácz Z.; Zrinyi, M. *J. Chem. Phys.* **1998**, *109*, 9479.

(9) Zrinyi, M.; Gálfi, L.; Smidróczki, É.; Rácz, Z.; Horkay, F. *J. Phys. Chem.* **1991**, *95*, 1618.

(10) Sultan, R.; Panjarian, S. *Physica D* **2001**, *157*, 241.

(11) Hilal, N.; Sultan, R. *Chem. Phys. Lett.* **2003**, *374*, 183.

(12) Das, I.; Pushkarna, A.; Agrawal, N. R. *J. Phys. Chem.* **1989**, *93*, 7269.

(13) Sultan, R.; Halabieh, R. *Chem. Phys. Lett.* **2000**, *332*, 331.

(14) Sultan, R.; Sadek, S. *J. Phys. Chem.* **1996**, *100*, 16912.

(15) Nasreddine, V.; Sultan, R. *J. Phys. Chem. A* **1999**, *103*, 2934.

(16) Shreif, Z.; Al-Ghoul, M.; Sultan, R. *ChemPhysChem* **2002**, *3*, 592.

(17) Sultan, R. F. *Phys. Chem. Chem. Phys.* **2002**, *4*, 1253.

(18) Al-Ghoul, M.; Sultan, R. *J. Phys. Chem. A* **2001**, *105*, 8053.

(19) Al-Ghoul, M.; Sultan, R. *J. Phys. Chem. A* **2003**, *107*, 1095.

(20) Polezhaev, A. A.; Müller, S. C. *Chaos* **1994**, *4*, 631.

(21) Ostwald, W. *Kolloid Z.* **1925**, *36*, 380.

(22) Büki, A.; Kárpáti-Smidróczki, É.; Zrinyi, M. *J. Chem. Phys.* **1995**, *103*, 10387.

(23) Büki, A.; Kárpáti-Smidróczki, É.; Zrinyi, M. *Physica A* **1995**, *220*, 357.